Research Article | Vol. 25, No. 20 | 2 Oct 2017 | OPTICS EXPRESS 23784

Optics EXPRESS

Silicon-organic hybrid (SOH) modulators for intensity-modulation / direct-detection links with line rates of up to 120 Gbit/s

HEINER ZWICKEL,[1] STEFAN WOLF,[1] CLEMENS KIENINGER,[1,2] YASAR KUTUVANTAVIDA,[1,2] MATTHIAS LAUERMANN,[1,3] TIMOTHY DE KEULENAER,[4,5] ARNO VYNCKE,[4,5] RENATO VAERNEWYCK,[4,5] JINGDONG LUO,[6] ALEX K.-Y. JEN,[6] WOLFGANG FREUDE,[1] JOHAN BAUWELINCK,[4] SEBASTIAN RANDEL,[1] AND CHRISTIAN KOOS[1,2,*]

[1]*Institute of Photonics and Quantum Electronics (IPQ), Karlsruhe Institute of Technology (KIT), Germany*
[2]*Institute of Microstructure Technology (IMT), Karlsruhe Institute of Technology (KIT), Germany*
[3]*Now with Infinera Corporation, Sunnyvale, CA 94089, USA*
[4]*Ghent University imec, IDLab, Department of Information Technology, Ghent, Belgium*
[5]*BiFAST, Ghent, Belgium*
[6]*Department of Material Science and Engineering, University of Washington, Seattle, Washington, USA*
[*]*christian.koos@kit.edu*

Abstract: High-speed interconnects in data-center and campus-area networks crucially rely on efficient and technically simple transmission techniques that use intensity modulation and direct detection (IM/DD) to bridge distances of up to a few kilometers. This requires electro-optic modulators that combine low operation voltages with large modulation bandwidth and that can be operated at high symbol rates using integrated drive circuits. Here we explore the potential of silicon-organic hybrid (SOH) Mach-Zehnder modulators (MZM) for generating high-speed IM/DD signals at line rates of up to 120 Gbit/s. Using a SiGe BiCMOS signal-conditioning chip, we demonstrate that intensity-modulated duobinary (IDB) signaling allows to efficiently use the electrical bandwidth, thereby enabling line rates of up to 100 Gbit/s at bit error ratios (BER) of 8.5×10^{-5}. This is the highest data rate achieved so far using a silicon-based MZM in combination with a dedicated signal-conditioning integrated circuit (IC). We further show four-level pulse-amplitude modulation (PAM4) at lines rates of up to 120 Gbit/s (BER = 3.2×10^{-3}) using a high-speed arbitrary-waveform generator and a 0.5 mm long MZM. This is the highest data rate hitherto achieved with a sub-millimeter MZM on the silicon photonic platform.

OCIS codes: (250.4110) Modulators; (060.2360) Fiber optics links and subsystems; (130.3120) Integrated optics devices; (230.2090) Electro-optical devices; (200.4650) Optical interconnects; (250.5300) Photonic integrated circuits.

References and links

1. J. D. Ambrosia and S. G. Kipp, "The 2015 Ethernet Roadmap," Ethernet Alliance White Paper (2015).
2. "IEEE P802.3bs 400 Gb/s Ethernet Task Force," http://www.ieee802.org/3/bs/.
3. D. M. Kuchta, "Directly modulated VCSELs at ≥50 Gb/s for short reach data communications," in *2016 IEEE Optical Interconnects Conference (OI)* (IEEE, 2016), paper MD1.
4. J. Verbist, M. Verplaetse, A. Srinivasan, P. De Heyn, T. De Keulenaer, R. Pierco, R. Vaernewyck, A. Vyncke, P. Absil, G. Torfs, X. Yin, G. Roelkens, J. Van Campenhout, and J. Bauwelinck, "First Real-Time 100-Gb/s NRZ-OOK Transmission over 2 km with a Silicon Photonic Electro-Absorption Modulator," in *Optical Fiber Communication Conference Postdeadline Papers* (OSA, 2017), paper Th5C.4.
5. M. Verplaetse, R. Lin, J. Van Kerrebrouck, O. Ozolins, T. De Keulenaer, X. Pang, R. Pierco, R. Vaernewyck, A. Vyncke, R. Schatz, U. Westergren, G. Jacobsen, S. Popov, J. Chen, G. Torfs, J. Bauwelinck, and X. Yin, "Real-Time 100 Gb/s Transmission Using Three-Level Electrical Duobinary Modulation for Short-Reach Optical Interconnects," J. Lightwave Technol. **35**(7), 1313–1319 (2017).
6. Y. Cheng, Q. J. Wang, and J. Pan, "1.55 μm high speed low chirp electroabsorption modulated laser arrays based

#301224 https://doi.org/10.1364/OE.25.023784
Journal © 2017 Received 29 Jun 2017; revised 23 Aug 2017; accepted 26 Aug 2017; published 19 Sep 2017

Optics EXPRESS

on SAG scheme," Opt. Express **22**(25), 31286–31292 (2014).
7. V. Katopodis, P. Groumas, Z. Zhang, R. Dinu, E. Miller, A. Konczykowska, J.-Y. Dupuy, A. Beretta, A. Dede, J. H. Choi, P. Harati, F. Jorge, V. Nodjiadjim, M. Riet, G. Cangini, A. Vannucci, N. Keil, H.-G. Bach, N. Grote, H. Avramopoulos, and C. Kouloumentas, "Polymer enabled 100Gbaud connectivity for datacom applications," Opt. Commun. **362**, 13–21 (2016).
8. P. Groumas, Z. Zhang, V. Katopodis, A. Konczykowska, J. Y. Dupuy, A. Beretta, A. Dede, J. H. Choi, P. Harati, F. Jorge, V. Nodjiadjim, M. Riet, R. Dinu, G. Cangini, E. Miller, A. Vannucci, N. Keil, H. G. Bach, N. Grote, M. Spyropoulou, H. Avramopoulos, and C. Kouloumentas, "Tunable 100 Gbaud Transmitter Based on Hybrid Polymer-to-Polymer Integration for Flexible Optical Interconnects," J. Lightwave Technol. **34**(2), 407–418 (2016).
9. S. Lange, S. Wolf, J. Lutz, L. Altenhain, R. Schmid, R. Kaiser, C. Koos, S. Randel, and M. Schell, "100 GBd Intensity Modulation and Direct Detection with an InP-based Monolithic DFB Laser Mach-Zehnder Modulator," in *Optical Fiber Communication Conference (OFC)* (OSA, 2017), paper Th5C.5.
10. Y. Ogiso, J. Ozaki, N. Kashio, N. Kikuchi, H. Tanobe, Y. Ohiso, and M. Kohtoku, "100 Gb/s and 2 V Vπ InP Mach-Zehnder modulator with an n-i-p-n heterostructure," Electron. Lett. **52**(22), 1866–1867 (2016).
11. Y. Ogiso, T. Yamada, J. Ozaki, Y. Ueda, N. Kashio, N. Kikuchi, E. Yamada, and H. Mawatari, "Ultra-High Bandwidth InP IQ Modulator with 1.5 V Vπ," in *European Conference on Optical Communications (ECOC)* (2016), paper Tu.3.A.4.
12. A. Samani, D. Patel, M. Chagnon, E. El-Fiky, R. Li, M. Jacques, N. Abadía, V. Veerasubramanian, and D. V. Plant, "Experimental parametric study of 128 Gb/s PAM-4 transmission system using a multi-electrode silicon photonic Mach Zehnder modulator," Opt. Express **25**(12), 13252–13262 (2017).
13. J. Fujikata, M. Noguchi, J. Han, S. Takahashi, M. Takenaka, and T. Nakamura, "Record-high Modulation-efficiency Depletion-type Si-based Optical Modulator with In-situ B Doped Strained SiGe Layer on Si Waveguide for 1.3 um Wavelength," in *European Conference on Optical Communications (ECOC)* (2016), paper Tu.3.A.4.
14. A. Samani, M. Chagnon, D. Patel, V. Veerasubramanian, S. Ghosh, M. Osman, Q. Zhong, and D. V. Plant, "A Low-Voltage 35-GHz Silicon Photonic Modulator-Enabled 112-Gb/s Transmission System," IEEE Photonics J. **7**(3), 1–13 (2015).
15. L. Chen, P. Dong, and Y.-K. Chen, "Chirp and Dispersion Tolerance of a Single-Drive Push–Pull Silicon Modulator at 28 Gb/s," IEEE Photonics Technol. Lett. **24**(11), 936–938 (2012).
16. A. Melikyan, K. Koehnle, M. Lauermann, R. Palmer, S. Koeber, S. Muehlbrandt, P. C. Schindler, D. L. Elder, S. Wolf, W. Heni, C. Haffner, Y. Fedoryshyn, D. Hillerkuss, M. Sommer, L. R. Dalton, D. Van Thourhout, W. Freude, M. Kohl, J. Leuthold, and C. Koos, "Plasmonic-organic hybrid (POH) modulators for OOK and BPSK signaling at 40 Gbit/s," Opt. Express **23**(8), 9938–9946 (2015).
17. C. Haffner, W. Heni, Y. Fedoryshyn, J. Niegemann, A. Melikyan, D. L. Elder, B. Baeuerle, Y. Salamin, A. Josten, U. Koch, C. Hoessbacher, F. Ducry, L. Juchli, A. Emboras, D. Hillerkuss, M. Kohl, L. R. Dalton, C. Hafner, and J. Leuthold, "All-plasmonic Mach-Zehnder modulator enabling optical high-speed communication at the microscale," Nat. Photonics **9**(8), 525–528 (2015).
18. C. Hoessbacher, A. Josten, B. Baeuerle, Y. Fedoryshyn, H. Hettrich, Y. Salamin, W. Heni, C. Haffner, C. Kaiser, R. Schmid, D. L. Elder, D. Hillerkuss, M. Möller, L. R. Dalton, and J. Leuthold, "Plasmonic modulator with >170 GHz bandwidth demonstrated at 100 GBd NRZ," Opt. Express **25**(3), 1762 (2017).
19. C. Koos, J. Leuthold, W. Freude, M. Kohl, L. Dalton, W. Bogaerts, A. L. Giesecke, M. Lauermann, A. Melikyan, S. Koeber, S. Wolf, C. Weimann, S. Muehlbrandt, K. Koehnle, J. Pfeifle, W. Hartmann, Y. Kutuvantavida, S. Ummethala, R. Palmer, D. Korn, L. Alloatti, P. C. Schindler, D. L. Elder, T. Wahlbrink, and J. Bolten, "Silicon-Organic Hybrid (SOH) and Plasmonic-Organic Hybrid (POH) Integration," J. Lightwave Technol. **34**(2), 256–268 (2016).
20. W. Hartmann, M. Lauermann, S. Wolf, H. Zwickel, Y. Kutuvantavida, J. Luo, A. K.-Y. Jen, W. Freude, and C. Koos, "100 Gbit/s OOK using a silicon-organic hybrid (SOH) modulator," in *European Conference on Optical Communications (ECOC)* (IEEE, 2015), paper PDP 1.4.
21. W. Heni, Y. Kutuvantavida, C. Haffner, H. Zwickel, C. Kieninger, S. Wolf, M. Lauermann, Y. Fedoryshyn, A. F. Tillack, L. E. Johnson, D. L. Elder, B. H. Robinson, W. Freude, C. Koos, J. Leuthold, and L. R. Dalton, "Silicon–Organic and Plasmonic–Organic Hybrid Photonics," ACS Photonics **4**(7), 1576–1590 (2017).
22. S. Koeber, R. Palmer, M. Lauermann, W. Heni, D. L. Elder, D. Korn, M. Woessner, L. Alloatti, S. Koenig, P. C. Schindler, H. Yu, W. Bogaerts, L. R. Dalton, W. Freude, J. Leuthold, and C. Koos, "Femtojoule electro-optic modulation using a silicon-organic hybrid device," Light Sci. Appl. **4**(2), e255 (2015).
23. C. Kieninger, Y. Kutuvantavida, H. Zwickel, S. Wolf, M. Lauermann, D. Elder, L. Dalton, W. Freude, S. Randel, and C. Koos, "Record-High In-Device Electro-Optic Coefficient of 359 pm/V in a Silicon-Organic Hybrid (SOH) Modulator," in *Conference on Lasers and Electro-Optics* (OSA, 2017), paper STu3N.2.
24. H. Zwickel, T. De Keulenaer, S. Wolf, C. Kieninger, Y. Kutuvantavida, M. Lauermann, M. Verplaetse, R. Pierco, R. Vaernewyck, A. Vyncke, X. Yin, G. Torfs, W. Freude, E. Mentovich, J. Bauwelinck, and C. Koos, "100 Gbit/s Serial Transmission Using a Silicon-Organic Hybrid (SOH) Modulator and a Duobinary Driver IC," in *Optical Fiber Communication Conference (OFC)* (OSA, 2017), paper W4I.5.
25. M. Scholten, T. Coe, and J. Dillard, "Continuously-Interleaved BCH (CI-BCH) FEC Delivers Best-in-Class NECG for 40G and 100G Metro Applications," in *National Fiber Optic Engineers Conference* (OSA, 2010), paper NTuB3.
26. H. Zwickel, S. Wolf, Y. Kutuvantavida, C. Kieninger, M. Lauermann, W. Freude, and C. Koos, "120 Gbit/s

Optics EXPRESS

PAM-4 Signaling Using a Silicon-Organic Hybrid (SOH) Mach-Zehnder Modulator," in *European Conference on Optical Communications (ECOC)* (2016), paper Th.2.P2.SC2.7.
27. R. Ding, T. Baehr-Jones, Y. Liu, R. Bojko, J. Witzens, S. Huang, J. Luo, S. Benight, P. Sullivan, J.-M. Fedeli, M. Fournier, L. Dalton, A. Jen, and M. Hochberg, "Demonstration of a low V π L modulator with GHz bandwidth based on electro-optic polymer-clad silicon slot waveguides," Opt. Express **18**(15), 15618–15623 (2010).
28. M. Lauermann, S. Wolf, W. Hartmann, R. Palmer, Y. Kutuvantavida, H. Zwickel, A. Bielik, L. Altenhain, J. Lutz, R. Schmid, T. Wahlbrink, J. Bolten, A. L. Giesecke, W. Freude, and C. Koos, "Generation of 64 GBd 4ASK signals using a silicon-organic hybrid modulator at 80°C," Opt. Express **24**(9), 9389–9396 (2016).
29. F. Devaux, Y. Sorel, and J. F. Kerdiles, "Simple measurement of fiber dispersion and of chirp parameter of intensity modulated light emitter," J. Lightwave Technol. **11**(12), 1937–1940 (1993).
30. S. Wolf, H. Zwickel, W. Hartmann, M. Lauermann, Y. Kutuvantavida, C. Kieninger, L. Altenhain, R. Schmid, J. Luo, A. K. Y. Jen, S. Randel, W. Freude, and C. Koos, "Silicon-Organic Hybrid (SOH) Mach-Zehnder Modulators for 100 Gbit/s On-Off Keying," submitted for publication (2017).
31. S. Wolf, H. Zwickel, W. Hartmann, M. Lauermann, Y. Kutuvantavida, C. Kieninger, L. Altenhain, R. Schmid, J. Luo, A. K. Y. Jen, S. Randel, W. Freude, and C. Koos, "Silicon-Organic Hybrid (SOH) Mach-Zehnder Modulators for 100 Gbit/s On-Off Keying–Supplementary Information," submitted for publication (2017).
32. Y. Ban, T. De Keulenaer, Z. Li, J. Van Kerrebrouck, J. H. Sinsky, B. Kozicki, J. Bauwelinck, and G. Torfs, "A Wide-Band, 5-Tap Transversal Filter With Improved Testability for Equalization up to 84 Gb/s," IEEE Microw. Comp. Lett. **25**(11), 739–741 (2015).
33. R. Ding, T. Baehr-Jones, W.-J. Kim, X. Xiong, R. Bojko, J.-M. Fedeli, M. Fournier, and M. Hochberg, "Low-loss strip-loaded slot waveguides in Silicon-on-Insulator," Opt. Express **18**(24), 25061–25067 (2010).
34. M. R. Watts, W. A. Zortman, D. C. Trotter, R. W. Young, and A. L. Lentine, "Low-Voltage, Compact, Depletion-Mode, Silicon Mach-Zehnder Modulator," IEEE J. Sel. Top. Quantum Electron. **16**(1), 159–164 (2010).
35. M. Lauermann, R. Palmer, S. Koeber, P. C. Schindler, D. Korn, T. Wahlbrink, J. Bolten, M. Waldow, D. L. Elder, L. R. Dalton, J. Leuthold, W. Freude, and C. Koos, "Low-power silicon-organic hybrid (SOH) modulators for advanced modulation formats," Opt. Express **22**(24), 29927–29936 (2014).
36. M. Lauermann, S. Wolf, P. C. Schindler, R. Palmer, S. Koeber, D. Korn, L. Alloatti, T. Wahlbrink, J. Bolten, M. Waldow, M. Koenigsmann, M. Kohler, D. Malsam, D. L. Elder, P. V. Johnston, N. Phillips-Sylvain, P. A. Sullivan, L. R. Dalton, J. Leuthold, W. Freude, and C. Koos, "40 GBd 16QAM Signaling at 160 Gb/s in a Silicon-Organic Hybrid Modulator," J. Lightwave Technol. **33**(6), 1210–1216 (2015).
37. S. Wolf, H. Zwickel, C. Kieninger, Y. Kutuvantavida, M. Lauermann, J. Lutz, L. Altenhain, R. Schmid, W. Freude, C. Koos, and S. Randel, "Silicon-Organic Hybrid (SOH) IQ Modulator for 100 GBd 16QAM Operation," in *Optical Fiber Communication Conference Postdeadline Papers* (OSA, 2017), paper Th5C.1.
38. P. J. Winzer and R.-J. Essiambre, "Advanced Optical Modulation Formats," Proc. IEEE **94**(5), 952–985 (2006).
39. L. Alloatti, R. Palmer, S. Diebold, K. P. Pahl, B. Chen, R. Dinu, M. Fournier, J.-M. Fedeli, T. Zwick, W. Freude, C. Koos, and J. Leuthold, "100 GHz silicon–organic hybrid modulator," Light Sci. Appl. **3**(5), e173 (2014).
40. L. Alloatti, D. Korn, R. Palmer, D. Hillerkuss, J. Li, A. Barklund, R. Dinu, J. Wieland, M. Fournier, J. Fedeli, H. Yu, W. Bogaerts, P. Dumon, R. Baets, C. Koos, W. Freude, and J. Leuthold, "42.7 Gbit/s electro-optic modulator in silicon technology," Opt. Express **19**(12), 11841–11851 (2011).
41. S. Wolf, M. Lauermann, P. Schindler, G. Ronniger, K. Geistert, R. Palmer, S. Kober, W. Bogaerts, J. Leuthold, W. Freude, and C. Koos, "DAC-Less Amplifier-Less Generation and Transmission of QAM Signals Using Sub-Volt Silicon-Organic Hybrid Modulators," J. Lightwave Technol. **33**(7), 1425–1432 (2015).
42. T. De Keulenaer, J. De Geest, G. Torfs, J. Bauwelinck, Y. Ban, J. Sinsky, and B. Kozicki, "56+ Gb/s serial transmission using duo-binary signaling," in *DesignCon* (2015), paper 10TH–3.
43. A. Lender, "The duobinary technique for high-speed data transmission," Trans. Am. Inst. Elec. Eng. Part I: Commun. Electron. **82**, 214–218 (1963).
44. A. Sekey, "An Analysis of the Duobinary Technique," IEEE Trans. Commun. **14**(2), 126–130 (1966).
45. J. Van Kerrebrouck, T. De Keulenaer, J. De Geest, R. Pierco, R. Vaernewyck, A. Vyncke, M. Fogg, M. Rengarajan, G. Torfs, and J. Bauwelinck, "100 Gb/s serial transmission over copper using duo-binary signaling," in *DesignCon* (2016).
46. P. Dong, J. Lee, Y. Chen, L. L. Buhl, S. Chandrasekhar, J. H. Sinsky, and K. Kim, "Four-Channel 100-Gb/s per Channel Discrete Multi-Tone Modulation Using Silicon Photonic Integrated Circuits," in *Optical Fiber Communication Conference (OFC)* (OSA, 2015), paper Th5B.4.

1. Introduction

High-speed optical communication links in data-center and campus-area networks urgently call for efficient high-speed electro-optic (EO) modulators that can be densely integrated at low cost. This need is, e.g., witnessed by the Ethernet Alliance, creating "The Holy Grail of 100GbE SFP+"-challenge that targets a single-wavelength 100 Gbit/s transceiver in a 1.5 W SFP + package (SFP: small form factor pluggable) [1]. This competition was driven by the expectation that grouping of 100 Gbit/s lanes will enable interface rates of 400 Gbit/s, 0.8 Tbit/s or 1.6 Tbit/s that are already foreseen for future Ethernet standards [2]. To meet the associated scalability challenges, system complexity must be kept low by using simple trans-

Optics EXPRESS

mission schemes based on intensity modulation and direct detection (IM/DD) as opposed to more demanding coherent communication schemes. In addition, due to growing areal network extension, the transmitters must be able to generate data signals with low chirp that can be sent over distances of up to a few kilometers. This rules out direct modulation concepts using, e.g., compact and efficient vertical-cavity surface-emitting lasers (VCSEL) [3], and requires external modulation of continuous-wave carriers.

External modulation schemes can rely on Mach-Zehnder modulators (MZM) or on electro-absorption modulators (EAM). EAM have been demonstrated both on the InP and the silicon photonic platform, enabling line rates of up to 100 Gbit/s with SiGe BiCMOS signal-conditioning chips [4,5]. However, EAM-based schemes generally suffer from a trade-off between extinction ratio (ER) and chirp, with typical chirp parameters α of experimentally generated data signals exceeding $|\alpha| > 1$ for an ER of 10 dB [6]. In contrast to that, MZM may feature arbitrarily high ER while allowing for push-pull operation with zero chirp. High-speed IM/DD transmission has previously been demonstrated using an MZM based on an organic EO polymer for 100 Gbit/s on-off-keying (OOK) [7,8]. While this device exploits the Pockels effect in the EO polymer to provide a negligible chirp parameter of $\alpha = -0.02$, it still features a large length in excess of 6 mm, dictated by the comparatively low EO coefficient of $r_{33} = 86$ pm/V as well as by the rather large optical mode field and the associated spacing of the microstrip transmission line electrodes. The device length can be slightly reduced to approximately 4 mm by using high-speed InP-based MZM [9,10]. These devices, however, still have rather high voltage-length products of more than 5 Vmm [11], and rely on fabrication processes that are rather expensive and limited in scalability as compared to CMOS-based silicon photonic integration. Silicon photonic depletion-type pn-modulators have been shown to support PAM4 signaling at impressive line rates up to 168 Gbit/s [12]. These devices, however, are subject to the intrinsically limited efficiency of the underlying phase modulators, featuring voltage-length products $U_\pi L$ in excess of 6 Vmm for optimized devices [13] and in excess of 30 Vmm [14] for the 4.8 mm-long high-speed MZM used in [12]. This leads to large device lengths and high drive voltages, which require dedicated amplifiers. Moreover, free carriers in the pn-junction do not only modulate the real part of the refractive index, but also the imaginary part, thereby leading to amplitude-phase coupling and hence to nonzero chirp parameters of, e.g., $|\alpha| = 0.8$ even for well-balanced push-pull devices [15]. Another approach to realize high-speed MZM relies on the concept of plasmonic-organic hybrid (POH) integration [16]. POH MZM combine ultra-small footprint [17] with unprecedented modulation bandwidths that enable data rates of up to 120 Gbit/s for PAM4 signaling [18]. These devices, however, suffer from an inherent trade-off between insertion loss and operation voltage [19], requiring peak-to-peak voltage swings of 8 V_{pp} that become effective when applying a 4 V_{pp} drive signal to an unterminated MZM [18]. In addition, with the exception of the all-polymer device [7,8], all signaling experiments of high-speed MZM have relied on drive signals generated by benchtop-type laboratory test equipment [9,10,18,20]. The associated electronic circuits feature high power consumption and are unsuited for integration into small form-factor packages.

In this paper, we present a series of IM/DD transmission experiments, showing that these limitations can be overcome by highly efficient silicon-organic hybrid (SOH) MZM, which can be operated by BiCMOS signal-conditioning chips. SOH modulators rely on silicon photonic slot waveguides that are embedded into organic EO cladding materials, thereby combining the advantages of large-scale CMOS fabrication with the wealth of optical properties obtained by molecular engineering of organic materials [19,21]. The devices feature small footprint along with low modulation voltages, quantified by small voltage-length products down to 0.32 Vmm [22,23] – more than an order of magnitude below those of conventional depletion-type pn modulators [13]. We characterize our SOH modulators with respect to ER and chirp and show that the devices can be operated with negligible chirp parameters of $|\alpha| = 0.09$. Moreover, expanding on earlier work [24], we demonstrate intensity-

Optics EXPRESS

modulated duobinary (IDB) as a way to relax the bandwidth requirements for driver electronics, modulators and receivers in IM/DD transmission schemes. We demonstrate 100 Gbit/s IDB transmission over a dispersion-compensated link of 5 km of standard single-mode fiber (SSMF) by operating an SOH MZM with a 130 nm SiGe BiCMOS signal-conditioning chip. We measure a bit error ratio (BER) of 1.6×10^{-3} (8.5×10^{-5}) for the fiber transmission (back-to-back reference), which is well below the threshold of hard-decision forward-error correction (FEC) with 7% overhead [25]. This represents, to the best of our knowledge, the highest data rate that has been achieved with a silicon-based MZM operated by a dedicated signal-conditioning chip. Moreover, we demonstrate generation of PAM4 signals at line rates (symbol rates) up to 120 Gbit/s (60 GBd) using a silicon-based modulator [26]. Despite the small device length of only 0.5 mm, the modulator's energy consumption amounts to W_{bit} = 100 fJ/bit, which is significantly smaller than the 410 fJ/bit demonstrated for a 4.8 mm long depletion-type modulator at a comparable PAM4 line rate of 112 Gbit/s [12]. To the best of our knowledge, our demonstration corresponds to the highest data rate hitherto achieved using a sub-millimeter MZM on the silicon photonic platform. The MZM are fabricated in a commercial silicon photonics line and along with the full portfolio of standard silicon photonic devices.

The paper is structured as follows: Section 2 introduces the SOH device concept and reports on the characterization of the MZM with respect to chirp. In Section 3, we explore OOK using SOH modulators in combination with integrated BiCMOS signal-conditioning chips, achieving error-free transmission at data rates of 50 Gbit/s. As a straightforward way to increase the data rates, we use PAM4 signaling at line rates of up to 120 Gbit/s. These experiments, reported in Section 4, however, rely on a high-speed arbitrary waveform generator that generates the multi-level drive signals. Section 5 finally introduces IDB as an alternative path towards high-speed signaling. IDB significantly relaxes the bandwidth requirements of the driver electronics, enabling data rates of up to 100 Gbit/s IDB with BiCMOS signal-conditioning ICs. Details on the modulation formats and the experimental methods are given in Appendix A and B.

2. Silicon-organic hybrid Mach-Zehnder modulator

The basic concept of a silicon-organic hybrid (SOH) Mach-Zehnder modulator (MZM) fabricated in silicon-on-insulator (SOI) technology is shown in Fig. 1(a). Each arm of the modulator consists of a silicon photonic slot waveguide, comprising two 240 nm wide and 220 nm high silicon rails which are separated by a 120 nm to 160 nm wide slot. The modulating drive signal is guided by a coplanar ground-signal-ground (GSG) aluminum (Al) transmission line. The modulating RF signal co-propagates with the optical carrier along the (0.5…1.1) mm long modulator. The electrodes are connected through Al vias to the silicon rails of the slot waveguide by 70 nm thin conductive n-doped silicon slabs. The electrical RF voltage drops mainly across the narrow slot where the light is highly confined, thus leading to a strong overlap of the optical mode and the modulating electric field – a key advantage in comparison to conventional organic electro-optic modulators [7,8]. The device is functionalized by filling and coating the slot waveguide with an EO organic cladding material.

This strip-loaded slot waveguide design clad with EO organic material was first demonstrated to work as an EO modulator at RF frequencies by Ding et al. [27]. We use the commercially available EO material SEO100 which combines a large EO coefficient of r_{33} = 144 pm/V with good thermal stability. Using this material, high-speed operation of an SOH modulator at 80 °C has been demonstrated previously [28]. To activate the macroscopic $\chi^{(2)}$- nonlinearity, the microscopic molecular dipoles in the organic material need to be aligned in a dedicated one-time poling process. To this end, a poling voltage U_{pol} is applied across the (floating) ground electrodes at an elevated temperature to align the EO-active chromophores. At the operating temperature and after removal of the poling voltage, the molecule orientation

Optics EXPRESS

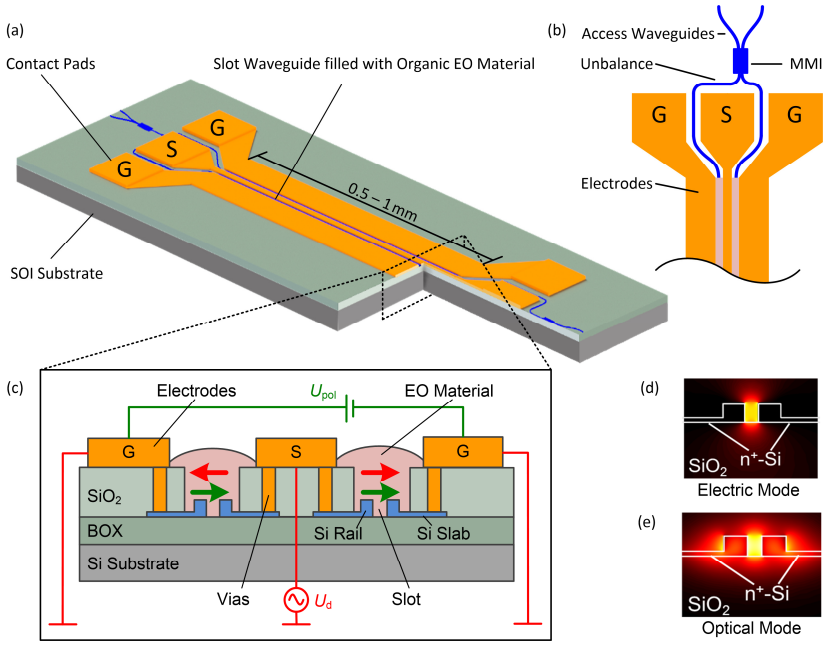

Fig. 1. Device concept of a silicon-organic hybrid (SOH) Mach-Zehnder modulator (MZM). (a) The device is fabricated in a standard commercial fabrication run on a silicon-on-insulator (SOI) wafer. (b) Shows a top view of the electrodes with contact pads in ground-signal-ground (GSG) configuration. The light is split by a multi-mode-interference coupler (MMI) into the two arms of the MZM. (c) Shows the cross section of the SOH MZM. Each arm comprises an optical slot waveguide filled with an electro-optic (EO) organic cladding material. The GSG transmission line for the electrical signal is connected to the rails of the slot waveguide by thin conductive n-doped silicon slabs and aluminum (Al) vias through the protective oxide cladding. During the poling process, a DC voltage U_{pol} (green circuit) is applied across the floating ground electrodes at an elevated temperature of the device. The molecules align according to the poling voltage and remain in that orientation (green arrow) after cooling down the device. A modulating voltage U_d applied to the signal electrode induces an electric field in the slot (red arrow) that is anti-parallel (parallel) in the left (right) arm of the MZM leading to push-pull operation. Due to the high overlap of the RF electric field (d) and the optical mode (e) in the slot waveguide the modulation is highly efficient.

remains in the aligned state indicated by green arrows, Fig. 1(c). The modulating field (red arrows) induced by the RF drive voltage U_d is oriented parallel to the chromophore alignment in one phase modulator and antiparallel in the other phase modulator, which results in a push-pull operation of the MZM. In the devices used for the transmission experiments, we measure an MZM voltage-length product $U_\pi L$ of 1.1 Vmm at DC. This value can be reduced to 0.5 Vmm or below by using more efficient EO materials [22,23]. Our devices were fabricated in a standard 248 nm deep-UV (DUV) process on a commercial platform, which offers a full portfolio of silicon photonic devices and SiGe detectors.

SOH MZM exploit the Pockels effects in the organic cladding and should hence allow for chirp-free modulation provided that perfectly balanced push-pull operation is achieved. To experimentally confirm this aspect, we characterized the chirp properties of an SOH MZM. In general, signal chirp is quantified by the chirp parameter α, which relates the modulation of the phase ϕ to the modulation of the time-dependent power P of the optical signal averaged over a few optical cycles,

$$\alpha = 2P\frac{\mathrm{d}\phi/\mathrm{d}t}{\mathrm{d}P/\mathrm{d}t}. \quad (1)$$

For a direct measurement of the chirp parameter, we exploit the fiber response peak

Optics EXPRESS

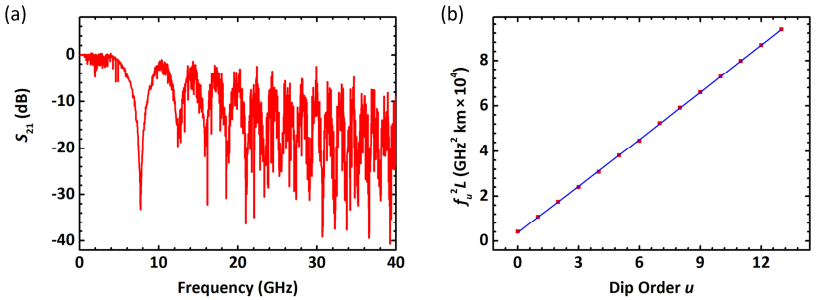

Fig. 2. Chirp characterization of an SOH Mach-Zehnder modulator using the fiber response peak method [29]. (a) Transfer function for small-signal intensity modulation of the SOH MZM connected to a 75 km-long fiber span. Dips in the transfer function originate from fiber dispersion. (b) For data evaluation, the product $f_u^2 L$ of the square of the resonance frequency f_u and the fiber length L is plotted versus the dip order u. The chirp parameter α and the fiber dispersion D can then be extracted from the slope and from the vertical offset of a straight line fitted to the data points [29–31]. We find a chirp factor of $|\alpha| \approx 0.09$.

method [29]. To this end, we use a network analyzer to measure the small-signal intensity modulation transfer function of the modulator connected to a 75 km-long fiber span and a calibrated photodiode [30]. The measured frequency response is shown in Fig. 2(a). The product $f_u^2 L$ of the square of the resonance frequency f_u and the fiber length L is plotted versus the dip order u in Fig. 2(b). The chirp parameter α and the fiber dispersion D can then be extracted from the slope and from the vertical offset of a straight line fitted to the data points by using the simple relation $f_u^2 L = c/(2D\lambda^2)\left(1+2u-2\arctan(\alpha)/\pi\right)$ with λ being the wavelength of the optical carrier and c denoting the vacuum speed of light [29]. Our measurements lead to a dispersion coefficient of 16.8 ps/(nm km) and a small but nonzero chirp parameter of $|\alpha| = 0.09$, which is attributed to a slight imbalance of the two MZM arms evidenced by a finite static ER of 31 dB, see [31]. The measured chirp parameter is well below the value of $|\alpha| = 0.8$ found for pn-type MZM [15] and significantly below the chirp parameters $|\alpha| > 1$ that are expected for EAM at reasonable extinction ratio [6].

3. Non-return-to-zero (NRZ) on-off keying (OOK) with an SOH MZM

In a first set of transmission experiments, we explore the potential of simple non-return-to-zero (NRZ) OOK as a modulation format. For generating the data signal, we bias the MZM at its quadrature point and apply a drive voltage with a swing of U_π. For rectangular pulses the data rate f_d equals the symbol rate f_s, and the required bandwidth is f_d (see Appendix A). While the electrical circuit to drive the MZM is relatively simple, OOK is demanding in terms of bandwidth so that it is challenging to move to high symbol rates. Recently, the generation and transmission of NRZ-OOK data at 100 Gbit/s using SOH modulators could be shown, where high-performance laboratory equipment controlled the modulator [20]. While this demonstration showed that SOH modulators outperform all alternative semiconductor based modulators in terms of speed and drive voltage, the implementation in a transmitter is rather complicated. First, the generation of electrical 100 Gbit/s signals requires components with high bandwidth. Second, the imperfect signal transmission (e.g. dispersion) requires error correction in the form of forward error correction (FEC), and this asks for digital signal processing (DSP).

In our experiment the 50 Gbit/s OOK signal is conditioned by an integrated circuit which

Optics EXPRESS

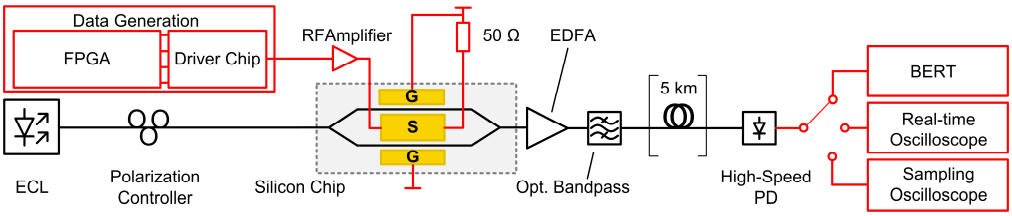

Fig. 3. Experimental setup for data transmission with an SOH modulator and an BiCMOS signal-conditioning IC: The signal-conditioning chip is fed by 4 × 12.5 Gbit/s or 4 × 25 Gbit/s pseudo-random binary sequences (PRBS) to generate a 50 Gbit/s on-off keying (OOK) signal or a 100 Gbit/s duobinary (DB) signal. The output of the IC connects via a coaxial cable to a radio-frequency (RF) amplifier and a microwave probe to the SOH Mach-Zehnder modulator. The modulator is terminated by a 50 Ω impedance. Light from a laser source is coupled to the silicon chip via grating couplers. After modulation, the optical signal is amplified, optionally transmitted over a 5 km long fiber and detected on a photodiode (PD). The PD can be connected to a bit error ratio tester (BERT), a sampling oscilloscope and a real-time oscilloscope.

comprises a 4:1 serializer, a 6-tap feed-forward equalizer (FFE), and an output stage delivering a voltage of up to 1 V_{pp}. The IC is fabricated in a 0.13 µm SiGe BiCMOS technology. The FFE is realized as a tapped delay line with around 9 ps to 10 ps spacing. More information on the signal-conditioning IC can be found in [5] and [32]. The experimental setup is depicted in Fig. 3. A pseudo-random binary sequence (PRBS, length $2^7 - 1$) is generated in a field-programmable gate array (FPGA) and feeds the signal-conditioning chip which is embedded in a connectorized testboard. The outputs of the board are connected to an RF amplifier with a bandwidth of 70 GHz, which finally drives the SOH MZM via microwave probes. The modulator is biased at its quadrature point and terminated with an external 50 Ω impedance. An external cavity laser (ECL) provides the optical carrier at a wavelength of 1550 nm. A band-pass filter with a 1.5 nm wide passband removes out-of-band amplified spontaneous emission (ASE) noise. The photodiode (PD) receives the transmitted signal. The PD output is connected to a bit error ratio tester (BERT), to a sampling oscilloscope, or to a 62 GHz real-time oscilloscope.

In our experiment, the optical signals are coupled to and from the silicon chip via grating couplers and single-mode fibers. The fiber-to-fiber insertion loss of 18 dB is compensated by an erbium-doped fiber amplifier (EDFA). This insertion loss is caused by non-optimized grating couplers, imperfect strip-to-slot waveguide transitions, and by waveguide losses. The on-chip loss amounts to approximately 9 dB, of which a total of approximately 2.5 dB is attributed to access waveguides, two MMI couplers, and four strip-to-slot converters. The remaining approximately 6.5 dB of loss are caused by the 1.1 mm long slot waveguide sections in each arm. With improved processes, the on-chip loss can be significantly reduced: Slot waveguides can be fabricated with propagation losses as low as 0.65 dB/mm [33], and an optimized doping profile can reduce the doping-related losses to below 1 dB/mm [28]. Note that this performance can well compete with the most advanced depletion-type pn modulators. First, the voltage-length product of $U_\pi L$ = 1.1 Vmm is significantly lower than $U_\pi L$-products of 6 Vmm that have been reported for advanced depletion-type pn-modulators. Moreover, despite the high slot-waveguide propagation losses of the current device generation, SOH modulators can well compete even with the most advanced depletion-type pn modulators in terms of the voltage-length-loss product $aU_\pi L$, where a denotes the waveguide loss coefficient in the phase shifter section: Best-in-class depletion-type pn modulators feature $aU_\pi L$-products down to 12 dBV [13], whereas 6.5 dBV are obtained for the SOH devices used in the current experiment, with the potential to reduce this value further

Optics EXPRESS

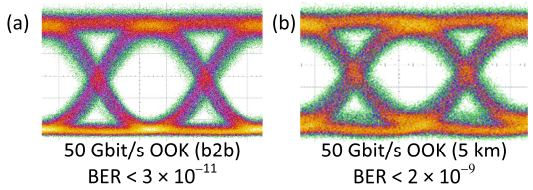

Fig. 4. Eye diagrams and BER for 50 Gbit/s OOK signaling. (a) Back-to-back (b2b) configuration (b) Transmission over a 5 km long dispersion compensated fiber.

to below 1 dBV. Regarding device capacitance, values of 400 fF/mm have been demonstrated for SOH modulators [22], which is clearly below the 830 fF/mm measured for highly efficient depletion-type pn devices [34]. This in combination with the higher modulation efficiency leads to clear advantages in terms of the charge that needs to be transferred to the device to achieve a certain phase shift, see [19] for a more detailed discussion.

Figure 4 shows eye diagrams recorded with a sampling oscilloscope. The BER is measured with a BERT. At 50 Gbit/s we find no errors in the data transmitted over a 5 km dispersion-compensated fiber link (evaluating 5×10^{10} bit, BER $< 2 \times 10^{-9}$). From the eye diagram we extract the quality factor (Q-factor) which is $Q = 7.0$. For a back-to-back measurement we find no errors in a data stream of 3.4×10^{12} bit (BER $< 3 \times 10^{-11}$) and a Q-factor of $Q = 10.3$. The energy consumption of the modulator is estimated to be 730 fJ/bit, see Appendix B. Note that the modulator itself would allow even higher data rates in the range of 100 Gbit/s if larger BER can be tolerated [20], and also the SiGe BiCMOS circuits can be pushed by a better optimization of the FFE coefficients [4]. However, in an integrated system, the electro-optic bandwidth will eventually be limited by the parasitic effects of the RF packagaging and assembly concepts. In the subsequent sections, we therefore explore two bandwidth-saving modulation formats for increasing the data rate.

4. Non-return-to-zero (NRZ) PAM4 signaling with an SOH MZM

To relax bandwidth requirements for the transmitter and the receiver, multilevel signaling can be employed. With PAM4, four signal levels are used to encode two bit into each symbol. For the same data rate f_d, the symbol rate and hence the bandwidth can be reduced by a factor of two as compared to OOK (see Appendix A). The required electronic circuitry for PAM4 is, however, more complex than for OOK due to multiple signal levels. For a proof-of-concept demonstration, we use an arbitrary waveform generator (AWG) rather than the BiCMOS IC.

The experimental setup is depicted in Fig. 5. The electrical drive signals are generated in a 92 GSa/s AWG (Keysight M8196A). An RF amplifier boosts the output to a peak-to-peak voltage of 2.1 V, which is fed to the Si chip using microwave probes. We use a pseudo-random binary sequence (PRBS) with a length of $2^{11}-1$ along with sinc-like pulse shapes featuring a raised-cosine spectrum with a roll-off factor $\beta = 0.35$. A pre-compensation flattens

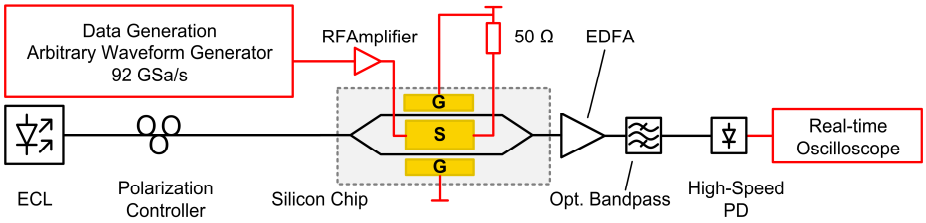

Fig. 5. Experimental setup for PAM4 signal generation: The electrical drive signals are generated in an arbitrary waveform generator (AWG), amplified in a radio frequency (RF) amplifier, and fed to the modulator via microwave probes. The modulator is electrically terminated with an external 50 Ω impedance. Light from a laser source is coupled to the chip via grating couplers. After modulation, the optical signal is amplified, bandpass filtered and detected on a photodiode (PD) connected to a high-speed oscilloscope.

Optics EXPRESS

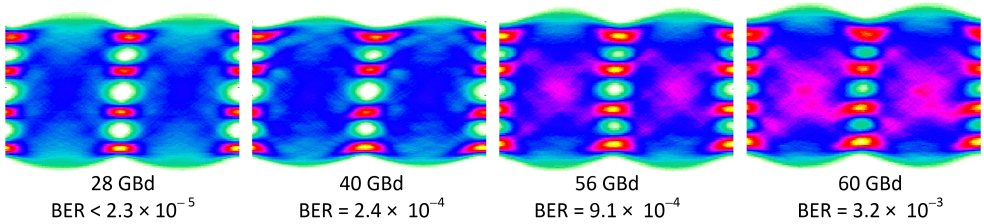

Fig. 6. PAM4 eye diagrams for symbol rates of 28 GBd, 40 GBd, 56 GBd and 60 GBd along with the measured bit error ratios (BER). At 28 GBd, no bit error was found in our recording. The BER increases with the symbol rate because the pre-compensation of the low-pass characteristic of driver electronics and modulator emphasizes high-frequency noise. For all measured symbol rates, the BER stays below 4.4×10^{-3}, which represents the threshold for hard-decision forward error correction (FEC) with 7% overhead.

the end-to-end frequency response of the setup. As with the previously described experiment, an external 50 Ω impedance terminates the electrical transmission line of the modulator. The optical carrier with a wavelength of 1550 nm is provided by an external cavity laser (ECL) and coupled to and from the 0.5 mm long SOH MZM via grating couplers. A subsequent erbium-doped fiber amplifier (EDFA) compensates the modulator's fiber-to-fiber insertion loss, and a 0.6 nm optical bandpass filter is used to remove the out-of-band amplified spontaneous emission (ASE) noise of the EDFA. The signal is detected by a photodiode having a bandwidth of 50 GHz. The data are then recorded by a real-time oscilloscope having a 32 GHz analog bandwidth. The BER is directly measured.

We demonstrate PAM4 modulation for symbol rates up to 60 GBd. The modulator is 0.5 mm long, biased at its quadrature point and driven with a voltage of 2.1 V_{pp}. Figure 6 shows the recorded eye diagrams with symbol rates of 28 GBd, 40 GBd, 56 GBd and 60 GBd. For the 28 GBd signal, no bit errors could be measured in our 78 µs long recordings, which corresponds to a BER < 2.29×10^{-5}. For 40 GBd, 56 GBd, and 60 GBd, the BER was measured to be 2.4×10^{-4}, 9.1×10^{-4} and 3.2×10^{-3}, respectively. The BER increases with increasing symbol rate because the pre-compensation of the low-pass characteristic of driver electronics and modulator emphasizes high-frequency noise. For all symbol rates, the BER is below the threshold 4.4×10^{-3} of hard-decision FEC with 7% overhead [25]. The maximum line rate is 120 Gbit/s, which corresponds to a net data rate of 112 Gbit/s. At the time of initial publication [26], this experiment represented the highest IM/DD data rate achieved on the silicon photonic platform. Despite the small device length of only 0.5 mm, the modulator's energy consumption amounts to W_{bit} = 100 fJ/bit, see Appendix B. This is significantly smaller than the 410 fJ/bit demonstrated for a 4.8 mm long depletion-type modulator at a comparable PAM4 line rate of 112 Gbit/s [12]. Note that even higher data rates can be achieved by using coherent transmission schemes along with advanced modulation formats such as 16-state quadrature amplitude modulation (16QAM) [35–37]. However, the associated transmitter and receiver circuitry is technically much more demanding than the rather simple IM/DD scheme used here, which does not require powerful DSP or coherent receivers. While the pre-emphasis used in our PAM4 demonstration as well as the coding and decoding of the four-level signal requires some DSP, the processing effort is much reduced compared to coherent modulation formats.

5. Demonstration of three-level intensity-modulated duobinary (IDB)

PAM4 signal generation and equalization requires complex signal processing schemes which prevent the construction of simple integrated driver chips. The data rate achieved with OOK, on the other hand, is limited by the bandwidth of the modulator and the driver electronics. To increase the line rate for a given bandwidth, we explore the bandwidth-saving duobinary (DB)

Optics EXPRESS

modulation format as alternative to PAM4, see Appendix A. With a setup change of the BiCMOS signal-conditioning chip in Fig. 3, three-level duobinary signals are generated. As with OOK, the modulator is biased at its quadrature point and driven with zero, positive and negative voltages. This leads to three optical power levels, which correspond to the signal levels (0, $A/2$, A) used in the Appendix. We refer to this format as intensity-modulated duobinary (IDB). Note that IDB is different from optical duobinary (ODB) [38], where the modulator is biased at the null-point, and the peak-to-peak drive signal swing U_{d} is twice the π-voltage U_{π} of the MZM. In ODB, the electrical three-level drive signal is converted into one zero and one non-zero optical power level, with a phase modulation of 0 and π for the non-zero levels. In contrast to ODB, the IDB signal is not optimum in terms of signal-to-noise power ratio and reach, but it allows bandwidth-saving signal processing in the electrical part of the transmitter and receiver.

Using the same devices as for the 50 Gbit/s OOK transmission, IDB transmission is demonstrated at a line rate of 100 Gbit/s. After opto-electric conversion with a photodiode, the received signal is recorded with a real-time oscilloscope at a sampling rate of 160 GSa/s. The BER is measured off-line without any equalization on the receiver side. Figure 7 shows the eye diagrams generated from the recordings for a back-to-back measurement, Fig. 7(a), and for transmission over a 5 km fiber link, Fig. 7(b). For the back-to-back measurement, the BER as extracted from the recordings is 4.3×10^{-4}, which can be improved to 8.5×10^{-5} by using a gate field of 0.1 V/nm to increase the conductivity of the doped silicons slabs of the SOH MZM [39]. In the current design, the gate field of 0.1 V/nm is created by a voltage that is applied to the silicon substrate and drops across the well-isolating, thick buried oxide layer. This requires a high static voltage of 200 V to maintain the gate field. The gate voltage can be reduced by using dedicated gate electrodes [40] or may even be completely omitted by using optimized doping profiles, both of which were not available for our experiments. Note that the gate voltage is not associated with any measurable current flow and does hence not lead to additional power dissipation in the device. After transmission over 5 km, the measured BER is 1.6×10^{-3}, clearly below the hard-decision FEC threshold 4.4×10^{-3} for 7% overhead. The estimated energy consumption of the modulator is 190 fJ/bit, assuming that the electrical energy is dissipated in the terminating resistor (see Appendix B). The signal-conditioning chip requires a power of 700 mW (incl. 4×25 Gbit/s multiplexer and 6-tap FFE) corresponding to 7 pJ/bit. Previously we showed that SOH modulators can be operated with peak-to-peak voltages well below 1 V_{pp} [41]. In a fully integrated package, the additional external drive amplifier can hence be omitted, and the total power consumption for the 100 Gbit/s transmittter will stay below 1 W. This is well compatible with the power ratings of highly compact SFP+ packages. Note that for our OOK and IDB experiments, signal processing comprises low-pass filtering performed by an “analog” equalizer that is directly implemented into the signal-conditioning IC and does not require digital operations, leaving aside any coding and decoding. The processing effort and the associated power consumption are hence expected to be much reduced compared to coherent modulation formats.

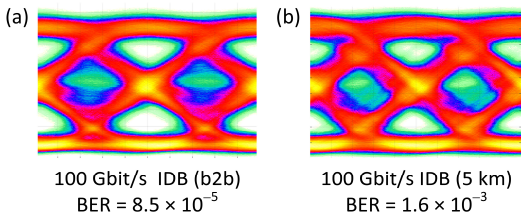

Fig. 7. Eye diagrams for 100 Gbit/s IDB signaling. The BER values stay below the FEC threshold 4.4×10^{-3} for 7% overhead. (a) Back-to-back (b2b) measurement (b) Transmission over a 5 km long dispersion-compensated fiber link.

Optics EXPRESS

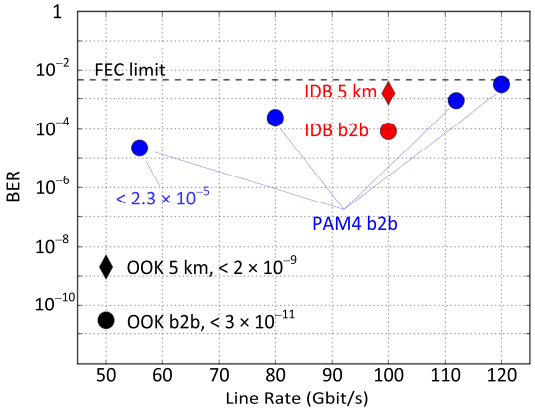

Fig. 8. Overview of all measured BER values for comparison. Dots represent the back-to-back (b2b) results for OOK (• black), PAM4 (• blue) and IDB (• red). For OOK and IDB the modulators were operated by a BiCMOS signal-conditioning IC and transmission over a 5 km dispersion compensated fiber link is shown (♦diamonds). Due to bandwidth limitations of the used components the BER increases with the data rate. All measured BER values stay below the threshold for FEC with 7% overhead. OOK at 50 Gbit/s is found to be error free.

6. Summary

Figure 8 recapitulates the BER for all performed experiments. Due to bandwidth and equipment limitations the BER increases with the line rate. PAM4 presents a viable method to push the line rate beyond 100 Gbit/s when powerful signal processing is available. In contrast to that, the simplicity of OOK and IDB modulation is attractive for integrated driver electronics that are subject to reasonable performance limitations. The excellent energy efficiency of SOH modulators and SiGe BiCMOS driver electronics holds promise for low cost and low power 100 G transmitters with small form factors. At 50 Gbit/s, error-free transmission could be demonstrated. No FEC is needed, which greatly simplifies the transceiver architectures. For 100 Gbit/s transmission using IDB modulation, the BER is below the threshold for hard-decision FEC with 7% overhead. The receiving circuit for IDB is comparatively simple and can be easily co-integrated with the modulator driver on a common transceiver chip [5]. Competing modulator concepts based on conventional pn-type silicon photonic devices, which are currently under development in the industry, struggle to fulfill the stringent requirements with respect to footprint and energy consumption that are associated with SFP modules. In contrast to that, the results of our 100 Gbit/s IDB experiments indicate that SOH modulators could be operated by integrated driver chips and allow for IM/DD transmission with disruptive power consumptions of less than 1 W. This represents an important step towards silicon photonic 100 Gbit/s and 400 Gbit/s transmitters compatible with SFP+ packages.

Appendix A

In this section we discuss three IM/DD modulation formats, namely non-return-to-zero on-off-keying (NRZ-OOK), 4-level pulse amplitude modulation (PAM4), and the duobinary (DB) format. We compare these modulation formats in terms of two main criteria: Spectral efficiency for a given bandwidth which is limited by optical and electronic components, and complexity of the required system, in particular the required electric circuitry and the bandwidth of the components, which has a direct impact on cost, scalability and energy consumption.

In the following discussion we consider rectangular non-return-to-zero (NRZ) pulses with identical peak signal level A. This signal can e.g. refer to a voltage, to a current, or to the

Optics EXPRESS

envelope of an optical power or intensity. A random bit stream is encoded into a sequence of pulses with a maximum height A.

Figure 9(a) shows an exemplary waveform for OOK. The pulse duration T is given by the symbol rate $f_s = 1/T$. Each symbol contains one bit of information, therefore the data rate f_d equals the symbol rate f_s. The spectrum of the random sequence of rectangular pulses is shown in Fig. 9(d) and is given by a sinc^2-function $\mathrm{sinc}^2\left(f/f_d\right)$. The first zero $f_d = 1/T$ of the power spectrum defines the bandwidth $B = f_d$ for the OOK signal. The level spacing of the signal equals A. The components at the receiver and transmitter side can be very simple as only binary signals are used. However, these components need to operate at high symbol rates, and therefore require a bandwidth in the order of f_d.

To relax bandwidth requirements, one can use multilevel signaling such as PAM4 where four signal levels are used to encode two bit into each symbol. Figure 9(b) shows the waveform of the same bit stream as in Fig. 9(a), now encoded with four signal levels 0, $A/3$, $2A/3$ and A, using Gray coding to map bit pairs into signal levels. For the same data rate f_d as with OOK, the symbol rate is now reduced by a factor of two. Because the pulse width doubles, the bandwidth of the $\mathrm{sinc}^2\left(f/\left(f_d/2\right)\right)$ decreases to $B = f_d/2$ (see Fig. 9(d)). However, the level spacing reduces by a factor of three and leads to a smaller eye-opening and more stringent signal-to-noise-ratio (SNR) requirements. While for PAM4 the electronics operates at half the OOK speed, the circuitry becomes significantly more complicated. On the transmitter side, binary inputs have to be converted into a four-level signal requiring a more complex equalizer and a linear driver. On the receiver side, three level slicers and a multi-level clock-and-data-recovery have to convert the signal back into a binary data stream.

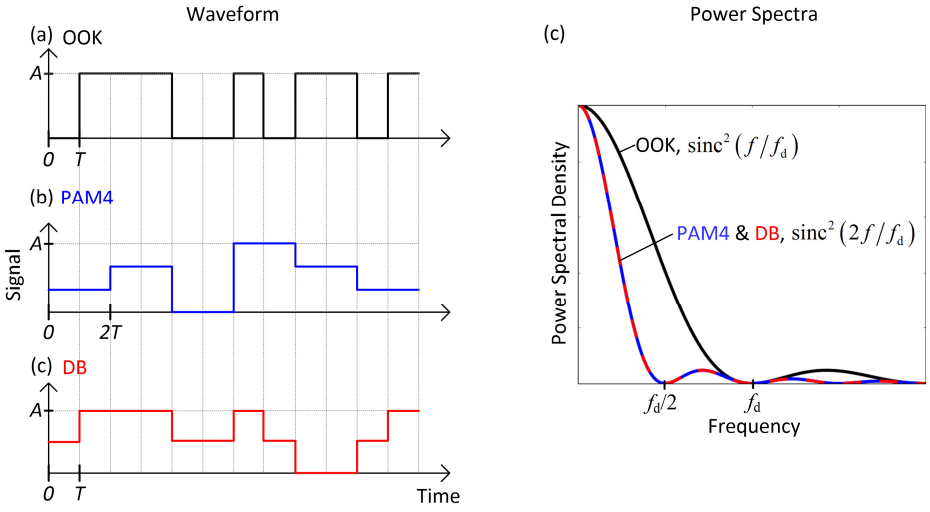

Fig. 9. Comparison of non-return-to-zero (NRZ) modulation formats and associated power spectra of random pulse sequences with a fixed data rate f_d. Because rectangular pulses are assumed, all spectra have a sinc^2-shape. Discrete spectral lines are disregarded. (a) Non-return-to-zero on-off keying (NRZ-OOK), (b) 4-level pulse amplitude modulation (PAM4), and (c) three level duobinary (DB), assuming rectangular pulse shapes and identical peak levels A. While OOK and DB operate at the same symbol rate $f_s = 1/T$, PAM4 encodes two bit per symbol so that the symbol rate can be halved, $f_s = 1/(2T)$. Duobinary signaling works with three signal levels and a (precoded) binary bit stream is encoded with a, e.g., delay-and-add-circuit. Therefore, starting from rectangular NRZ pulses the DB correlation time is doubled as compared to OOK, and the bandwidth is halved. Since for the same average power the distance between neighboring PAM4 and DB levels is reduced as compared to OOK, the noise tolerance is reduced.

Optics EXPRESS

An alternative approach to narrow down the spectrum without decreasing the symbol rate is the use of partial response signaling (PR). In PR signaling schemes, the data to be transmitted are distributed over multiple symbols [42]. A particularly interesting PR format is duobinary modulation (DB) as presented by Lender [43] and Sekey [44]. This format operates at the full OOK symbol rate but encodes one bit per symbol into three levels. A logical "0" is represented by the middle level; and a logical "1" is represented by either the upper or the lower level, depending on the number of logical "0" between two logical "1" [43]: If a logical "1" is represented by an upper (lower) level and an odd number of logical "0" follows, then the next logical "1" is represented by the lower (upper) level. If the number of logical "0" between two logical "1" is even, then the subsequent logical "1" is represented by the previous "1" level. The procedure introduces a correlation between two consecutive symbols, and for a random sequence, the correlation time $2T$ is doubled as compared to OOK with a correlation time of T. The power spectrum of a random data sequence is again a sinc^2-function, but with a bandwidth $B = f_\mathrm{d}/2$ [44]. This statement holds for rectangular symbols. The DB spectrum shown in Fig. 9(d) is identical with the PAM4 spectrum of the PAM4 signal at the same data rate.

The DB coding can be realized by a pre-coded binary bit stream and a simple delay-and-add circuit, or by a low-pass filter with a bandwidth that resembles the same frequency response as the delay-and-add circuit [42,45]. Duobinary coding is easy to implement, and even the low-pass characteristic of the transmission channel itself can be used to convert a (precoded) OOK signal into a DB format [45]. Thus, the advantage of a reduced transmission bandwidth does not come at the cost of complicated electronics as with PAM4. At the transmitter, the natural frequency roll-off, often combined with an equalizer can be used to generate the DB signal from an OOK signal. At the receiver two slicers and an XOR-circuit are sufficient to recover the binary data stream [42]. The DB level spacing is $A/2$ and therefore DB is less noise tolerant than OOK, but more resilient than PAM4.

A special case of DB often employed in optical transmission systems is most commonly referred to as optical duobinary (ODB). In ODB, the three levels in the electrical signal are modulated onto an optical carrier such that the optical signal has two intensity levels like OOK, but an additional phase modulation. This gives an advantage in SNR but restricts the bandwidth saving effect of DB to the transmitter. In contrast to that, our experiment relies on three signal levels that are represented by three optical intensities, and we refer to the scheme as intensity-modulated duobinary (IDB). We feel that this nomenclature is more precise than the often used naming electrical DB (EDB). Intensity-modulated duobinary is advantageous because the electro-optic modulator requires only half the drive voltage swing than with ODB, and because electronic bandwidth requirements are relaxed both at the transmitter and at the receiver side.

As an alternative to the presented modulation formats, it is possible to exploit multicarrier formats such as discrete multitone (DMT) transmission, also known as orthogonal frequency multiplexing (OFDM), in an IM/DD transmission scheme [46]. While the spectral efficiency would be better, these schemes require high-speed DACs, ADCs and digital signal processing (DSP), which are associated with significant power consumption and technical complexity. Such schemes and are not considered in our work, which focusses on cost and power-efficient solutions for short reach optical interconnects.

Table 1 summarizes the key advantages and disadvantages of OOK, PAM4 and IDB. We show that SOH modulators are suited for all three formats.

To get a more quantitative idea about the SNR tolerance of the three modulation formats we estimate the BER of a rectangular NRZ signal. To this end, we consider the voltage after detection with a photodiode. The lowest signal voltage is 0 and the highest voltage is A as depicted in Fig. 9. We assume equidistant signal levels, and Gray coding for the case of PAM4. The decision thresholds are placed in the center between two adjacent levels. Further,

Optics EXPRESS

Table 1. Comparison of OOK, PAM4 and IDB modulation formats

Modulation format	Pros	Cons
OOK	• Simple modulator drive electronics • Simple receiver architecture (1 slicer) • Large eye opening	• Demanding bandwidth requirement for electronics
PAM4	• Reduced bandwidth requirements • Operation at half the OOK symbol rate	• Complex drive and receiver electronics (3 slicers) • Reduced eye opening (1/3 of OOK)
IDB	• Reduced bandwidth requirement • Simple drive and receiver electronics	• Operation at full OOK symbol rate • Reduced eye opening (1/2 of OOK)

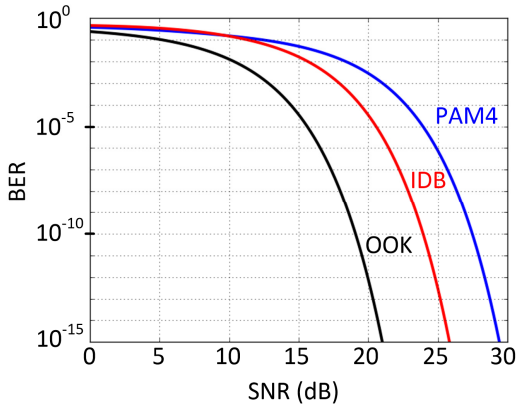

Fig. 10. Bit error ratio (BER) calculated by Eq. (2) for the modulation formats on-off keying (OOK), 4-level pulse amplitude modulation (PAM4), and intensity-modulated duobinary (IDB) signaling as a function of the electrical signal-to-noise power ratio (SNR). Equal electrical peak powers are assumed, leading to the best noise tolerance for two level OOK. The level spacing becomes smaller for IDB (three signal levels) and PAM4 (four signal levels), and the noise tolerance worsens. For PAM4 we use Gray coding.

we assume additive white Gaussian noise with an average electrical power $P_{\mathrm{N}} = \sigma^2$ equal to the noise variance σ^2 for all signal levels. The following BER result:

$$\begin{aligned}
\mathrm{BER}_{\mathrm{OOK}} &= \frac{1}{2}\mathrm{erfc}\left(\frac{A}{2\sqrt{2}\sigma}\right), \\
\mathrm{BER}_{\mathrm{PAM4}} &= \frac{3}{8}\mathrm{erfc}\left(\frac{A}{6\sqrt{2}\sigma}\right) + \frac{1}{4}\mathrm{erfc}\left(\frac{3A}{6\sqrt{2}\sigma}\right) - \frac{1}{8}\mathrm{erfc}\left(\frac{5A}{6\sqrt{2}\sigma}\right) \approx \frac{3}{8}\mathrm{erfc}\left(\frac{A}{6\sqrt{2}\sigma}\right), \quad (2) \\
\mathrm{BER}_{\mathrm{IDB}} &= \frac{3}{4}\mathrm{erfc}\left(\frac{A}{4\sqrt{2}\sigma}\right) - \frac{1}{4}\mathrm{erfc}\left(\frac{3A}{4\sqrt{2}\sigma}\right) \approx \frac{3}{4}\mathrm{erfc}\left(\frac{A}{4\sqrt{2}\sigma}\right).
\end{aligned}$$

The complementary error function is defined by $\mathrm{erfc}(z) = \left(2/\sqrt{\pi}\right)\int_z^\infty \exp(-t^2)\mathrm{d}t$. We compare these modulation formats for identical optical average powers which happen to result in identical optical peak powers and therefore identical electrical peak powers A^2. However, the average electrical signal power measured after the photodiode differ,

$$P_{\mathrm{S\,OOK}} = \frac{A^2}{2}, \qquad P_{\mathrm{S\,PAM4}} = \frac{7A^2}{18}, \qquad P_{\mathrm{S\,IDB}} = \frac{3A^2}{8}. \quad (3)$$

We define the electrical signal-to-noise power ratio by $\mathrm{SNR} = P_{\mathrm{S}}/P_{\mathrm{N}}$. Figure 10 shows a plot of the BER as a function of the SNR.

Optics EXPRESS

The modulation format with the widest level spacing (OOK, level spacing = A) is most tolerant to noise. As the signal spacing is reduced for IDB (level spacing = $A/2$) and for PAM4 (level spacing = $A/3$), the probability to receive erroneous bits increases, and the BER for a given SNR becomes larger.

Appendix B

To estimate the power consumption of the SOH modulator, we assume that the travelling-wave electrodes are represented by ideal transmission lines which are perfectly matched at both ends. The terminating AC-coupled load resistance is R. The applied drive voltage drops across the terminating resistor, and the modulation signal power is entirely dissipated in the load. The modulator bias voltage fixes the MZM operating point at the quadrature point and is irrelevant for energy considerations because of the AC-coupling of the terminating resistor R. The drive voltage supplied by the amplifier was either directly measured or estimated from the specifications of the amplifier. This estimation of the energy consumption takes only account of the energy dissipated in the modulator's terminating resistor.

For OOK with a data rate r_{OOK}, with binary rectangular signals, equiprobable "ones" and "zeros", and for a DC-free electrical drive signal with a peak-to-peak voltage swing U_{d}, we write for the energy dissipated per bit

$$W_{\mathrm{bit\,OOK}} = \frac{(U_{\mathrm{d}}/2)^2}{50\,\Omega}\frac{1}{r_{\mathrm{OOK}}}. \tag{4}$$

The 3-level signal for intensity-modulated duobinary is made up from a state with $U = 0$ corresponding to a representation of a "zero" of the binary signal and $U = \pm U_{\mathrm{d}}/2$ representing a "one". For the energy dissipated per bit we therefore find the expression

$$W_{\mathrm{bit\,IDB}} = \frac{1}{2}\frac{(U_{\mathrm{d}}/2)^2}{50\,\Omega}\frac{1}{r_{\mathrm{IDB}}}. \tag{5}$$

The 4-level PAM4 signal consists of the equiprobable states $U = \pm U_{\mathrm{d}}/2$ and $U = \pm U_{\mathrm{d}}/6$. The energy consumption per bit is

$$W_{\mathrm{bit\,PAM4}} = \frac{1}{2}\left[\frac{(U_{\mathrm{d}}/2)^2}{50\,\Omega} + \frac{(U_{\mathrm{d}}/6)^2}{50\,\Omega}\right]\frac{1}{r_{\mathrm{PAM4}}}. \tag{6}$$

Table 2 gives a summary of the modulator data for the various experiments including the energy consumption per bit.

Table 2. Overview of modulator data for three experiments. A DC voltage in the range 0V…U_π for setting the operating point was applied in all measurements.

Line Rate	Modulation Format	Modulator length	π-Voltage	Peak-to-Peak Voltage	Energy/bit
50 Gbit/s	OOK	1.1 mm	1.2 V	2.7 V_{pp}	730 fJ/bit
100 Gbit/s	IDB	1.1 mm	1.2 V	2.8 V_{pp}	190 fJ/bit
120 Gbit/s	PAM4	0.5 mm	2.2 V	2.1 V_{pp}	100 fJ/bit

Funding

European Research Council (ERC Starting Grant 'EnTeraPIC', 280145 and the ERC Proof-of-Concept Grant 'SCOOTER', 755380); EU-FP7 projects PhoxTroT (318240) and BigPipes (619591); Alfried Krupp von Bohlen und Halbach Foundation; Helmholtz International Research School for Teratronics (HIRST); Karlsruhe School of Optics and Photonics (KSOP); Karlsruhe Nano-Micro Facility (KNMF).

Optics EXPRESS

Acknowledgments

The 100 Gbit/s driver chips have been developed by the BiFast spin-off incubation project, funded by the industrial research fund (IOF) of Ghent University.